


 Cite this: *RSC Adv.*, 2022, 12, 31180

Polymers based on thieno[3,4-*c*]pyrrole-4,6-dione and pyromellitic diimide by CH–CH arylation reaction for high-performance thin-film transistors†

 Gamal M. Nassar,^{‡ab} Jeyon Chung,^{‡c} Cuc Kim Trinh,^{ib} ‡^d Ashraf A. El-Shehawy,^e Ahmed A. El-Barbary,^{*b} Youngjong Kang^{ib} *^c and Jae-Suk Lee^{ib} *^a

Three homopolymers were successfully synthesized by direct CH–CH arylation polymerization of thieno[3,4-*c*]pyrrole-4,6-dione or pyromellitic diimide derivatives affording highly purified polymers with high molecular weights (43.0–174.7 K). Thieno[3,4-*c*]pyrrole-4,6-dione and pyromellitic diimide derivatives are considered as electron-withdrawing units. The synthesized homopolymers P1, P2, and P3 showed band gaps in the range of 2.13–2.08 eV, respectively. The electron mobilities of the three homopolymers have been investigated. The thin film transistor for P1 prepared by the eutectic-melt-assisted nanoimprinting method achieved an electron mobility of $2.11 \times 10^{-3} \text{ cm}^2 \text{ s}^{-1} \text{ V}^{-1}$. Based on the obtained results, the synthesized polymers can be used as potential electron acceptors in solar cell applications.

 Received 24th July 2022
 Accepted 24th October 2022

DOI: 10.1039/d2ra04602d

rsc.li/rsc-advances

Introduction

Several synthetic methodologies including electrochemical,^{1–3} chemical oxidative^{4–6} and transition metal-catalyzed cross-coupling reactions^{7–10} have been investigated for the synthesis of π -conjugated organic and polymeric materials. Direct C–H arylation reaction has been proved to be a particularly efficient methodology for the formation of carbon–carbon bonds without the use of organometallic nucleophiles.^{11–22} Direct arylation reactions have been reported by many researchers including our group,^{15–22} and proven to be useful for synthesizing a variety of π -conjugated polymers with high molecular weights. In the past decade, comprehensive efforts have been made on transition metal (*e.g.*, Pd and Fe) catalysed oxidative coupling on arenes.^{23–25} Very recently, transition metal-free

oxidation acylation of arenes has shown a promising method for oxidative acylation of different heteroarenes.^{26,27} Oxidative coupling of C–H bonds without prior functionalization is an environmentally friendly, step-economically, and sustainable method.^{28–30}

During the last decade, the performance of organic thin-film transistors (OTFT) has advanced dramatically with the charge carrier mobility (μ) and now approaching $100 \text{ cm}^2 \text{ V}^{-1} \text{ s}^{-1}$.^{31,32} While there are a variety of p-type organic semiconductors, n-type materials are relatively limited. PCBM has been widely used as an acceptor owing to its excellent electron-accepting and electron-transporting properties.^{33,34} However, PCBM has relatively low absorption in the visible and near-IR. The use of acceptor polymers with improved light absorption has met with limited success.^{35,36} To improve OTFT applications, other n-type acceptors with suitable properties such as high absorption and high oxidation resistance are still highly demanded.³⁷ In addition, to enhance optical and electrical properties, many groups have tried to improve organic semiconductors' crystallinity with a controlled crystal structure. However, the highly crystalline polymers has low solubility which will hamper device fabrication by using the conventional methods. Therefore, in this paper, the eutectic-melt-assisted nanoimprinting (EMAN) method was applied to fabricate optoelectronic devices based on highly crystalline polymers instead of solution casting techniques.³⁸ Nanoimprinting technique is one of the most convenient production processes because of its advantages such as cost-effective, scalable production and obtained high-resolution structures, *etc.*³⁹

^aSchool of Materials Science and Engineering, Gwangju Institute of Science and Technology (GIST), 123 Cheomdangwagi-ro, Buk-gu, Gwangju 61005, Korea. E-mail: jslee@gist.ac.kr

^bDepartment of Chemistry, Faculty of Science, Tanta University, Tanta 31527, Egypt. E-mail: aelbarbary@hotmail.com

^cDepartment of Chemistry, Institute of Nano-Science and Technology and Research Institute for Natural Sciences, Hanyang University, Wangsimni-Ro, Seongdong-Gu, Seoul, 04763, Korea. E-mail: youngjkang@hanyang.ac.kr

^dChemical Engineering in Advanced Materials and Renewable Energy Research Group, School of Engineering and Technology, Van Lang University, Ho Chi Minh City, Vietnam

^eDepartment of Chemistry, Faculty of Science, Kafrelsheikh University, Kafrelsheikh 33516, Egypt

† Electronic supplementary information (ESI) available. See DOI: <https://doi.org/10.1039/d2ra04602d>

‡ These authors contributed equally to this work.



Herein, we wish to report on the Pd(II)-catalyzed regioselective direct CH–CH arylation coupling reaction for the synthesis of some polymers based on thieno[3,4-*c*]pyrrole-4,6-dione and pyromellitic diimide with high molecular weights (43.0–174.7 K), which can be used as n-type semiconducting materials. The direct heteroarylation polycondensation reaction provides an environmentally friendly and fast route with minimal reaction steps.^{40–44} The catalytic CH–CH direct arylation coupling of two heteroarenes represents a promising advance in organic chemistry and the synthesis of small molecules.^{45,46} Dimethylformamide (DMF) was essentially used as a reaction solvent as it has been proved particularly to be effective for obtaining high catalytic activity.^{47,48} In addition, the electron mobility of the homopolymer P1-based FET device has successfully been fabricated by the eutectic-melt-assisted nanoimprinting (EMAN) method^{49,50} and its thin-film transistor has achieved electron mobility is $2.11 \times 10^{-3} \text{ cm}^2 \text{ V}^{-1} \text{ s}^{-1}$.

Experimental

Instruments and measurements

All manipulations and reactions involving air-sensitive reagents were performed under a dry oxygen-free nitrogen atmosphere. All ¹H- and ¹³C-NMR spectra were measured on a Varian spectrometer (400 MHz for ¹H-NMR and 100 MHz for ¹³C-NMR) in CDCl₃ at 25 °C with TMS as the internal standard. Chemical shifts were recorded in ppm units. The gel permeation chromatography (GPC) analysis was conducted with Shimadzu (LC-20A prominence Series) instrument. Chloroform was used as a carrier solvent (flow rate: 1 ml min⁻¹ at 40 °C) and calibration curves were made with standard polystyrene samples.

Materials

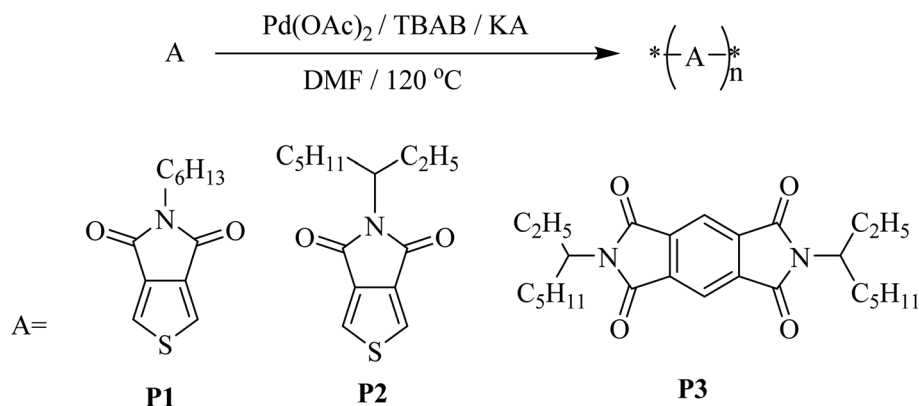
All reagents and solvents were obtained from commercial sources and dried using standard procedures before use. Pyromellitic acid diimide, palladium acetate, and potassium acetate were obtained from Sigma-Aldrich. Tetrabutylammonium bromide (TBAB) was obtained from TCI Company. Thiophene-3,4-dicarboxylic acid was obtained from Matrix Scientific. All reactions were monitored by TLC to follow their completion.

General procedure for the synthesis of homopolymers P1, P2 and P3

Under a nitrogen atmosphere, potassium acetate (2.26 mmol), tetrabutylammonium bromide (0.75 mmol), and palladium acetate (0.037 mmol) were added to a stirred solution of starting material (0.37 mmol) in anhydrous DMF (7 ml). The resulting suspension was heated under reflux for 48 h at 120 °C. The reaction mixture was cooled to room temperature and then poured into methanol. The crude polymer was collected *via* filtration and washed successively with methanol. The residual solid was loaded into an extraction thimble and washed repeatedly with methanol (48 h), hexane (48 h), followed by acetone (48 h) followed by drying under vacuum affording the desired polymer. For more details, see ESI.†

General fabrication of FET devices

FET devices were fabricated by the eutectic-melt-assisted nanoimprinting (EMAN) method.^{49–54} Briefly, the powder mixtures of each polymer (P1, P2, and P3) and 1,4-DBTFB (polymer = 2 wt%) were first placed on a substrate and covered with a PDMS mask. The sample was then heated to melt the powder completely. At this time, the molten liquid was sucked into the grooves of the PDMS mold by the capillary force. The extra liquid was removed by soaking out using paper. The sample was cooled down to room temperature. After removing the PDMS mold, the sample was placed in a vacuum to remove 1,4-DBTFB. The resulting polymer wires were transferred on a highly doped p-type silicon wafer (100) with a thermally grown 200 nm thick oxide layer using a liquid-bridge-mediated nano transfer molding (LB-nTM) method.⁴⁹ By using LB-nTM, the laterally aligned P1 wires can be transferred to the hydrophilic SiO₂ substrate. Finally, 200 nm thick gold electrodes separated by 100 μm were vacuum deposited through a shadow mask on the P1 wire patterns. Current–voltage (*I*–*V*) characteristics of the devices were measured using bottom-gate FET geometry under the ambient conditions at room temperature, and the saturation regime mobility was calculated. FET devices based on P2 and P3 did not properly work due to poor film morphology or poor adhesion property.



Scheme 1 Synthesis of the polymers by CH–CH arylation polymerization.



Results and discussion

Synthesis of homopolymers P1, P2 and P3

The synthesis of some π -conjugated homopolymers and their electron mobilities properties have been investigated. Thieno [3,4-*c*]pyrrole-4,6-dione derivatives with electron-withdrawing groups having good arrangement and planarity have been used. We successfully synthesized some homopolymers in a few steps, at low cost, and with good charge mobility. 5-Hexyl-thieno [3,4-*c*]pyrrole-4,6-dione (HTPD), 5-(2-ethylhexyl)thieno[3,4-*c*]pyrrole-4,6-dione (ETPD) and 1,5-di(2-ethylhexyl)-pyromellitic diimide (EPDI) were selected to be used for the synthesizing the target homopolymers. All the homopolymers were synthesized by CH-CH arylation polymerization (Scheme 1).

In CH-CH arylation polymerization, the unsubstituted positions which are highly reactive by the presence of electron-withdrawing and/or electron-donating group can be activated by the catalyst in the presence of a highly polar solvent such as DMF, DMAC, or DMSO to start the polymerization giving a high molecular weight polymer in good yield. For instance, polymer P1 could be obtained with a high yield (70%) and a high molecular weight ($M_n = 174$ K). The polymer P2 was also successfully prepared by the same CH-CH arylation method with lower yield (50%) and lower molecular weight ($M_n = 70.5$ K) when compared to those corresponding values obtained for polymer P1. This is probably due to the effect of the branched alkyl chain which reduces the planarity of the polymer despite the presence of the imide group which makes the 3,4-positions on thiophene ring very active. Furthermore, EPDI derivative could also be polymerized under the present methodology of CH-CH arylation conditions affording the desired homopolymer P3 with a yield of 49% and M_n value of 43.0 K (PDI = 1.5). Interestingly, polymer P3 showed lower M_n values when compared to is less than P1 in the M_n because the reactivity of the thiophene ring is higher than the benzene ring so this affected gradually the reactivity of the unsubstituted 4,9 positions on the benzene ring in EPDI. The optimized condition for all the polymers and their high molecular weights and PDI are shown in Table 1. However, the molecular weights and PDI values were measured by gel permeation chromatography (GPC).

Table 1 Chemical yields and GPC data for the synthesis of π -conjugated homopolymers^a

Entry	Polymer	M_n^b (kDa)	PDI (M_w/M_n^b)	Yield ^c (%)
1	P1	174.7	1.3	70
2	P2	70.5	1.2	50
3	P3	43.0	1.5	49

^a All polymers were prepared *via* CH-CH arylation in presence of Pd(OAc)₂ (10 mol%) as a catalyst in DMF at 120 °C for 48 h. ^b GPC calibration based on polystyrene standards using CHCl₃ as the mobile phase, M_n = number average molecular weight, PDI = polydispersity index. ^c Based on the weight of pure polymers obtained after Soxhlet extraction followed by drying under vacuum for 24 h.

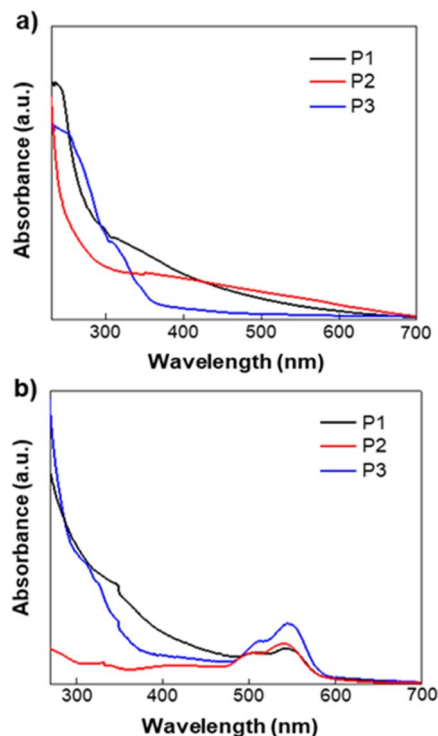


Fig. 1 UV-vis absorption spectra of P1, P2 and P3 (a) in solution and (b) as casted film. Chloroform was used as the solvent.

Optical and electrochemical properties of homopolymers P1, P2 and P3

The optical properties of homopolymers P1, P2 and P3 were investigated by UV-vis absorption spectroscopy for both solution and thin films (Fig. 1). As shown in Fig. 1, the polymers P1, P2 and P3 show similar absorption UV-vis spectra with narrow absorption at short wavelengths, giving almost similar optical bandgaps. P3 shows λ_{onset} in the solid-state is ~ 593.5 nm, which is ~ 10 nm red-shifted compared to that of P1 (~ 581 nm) and P2

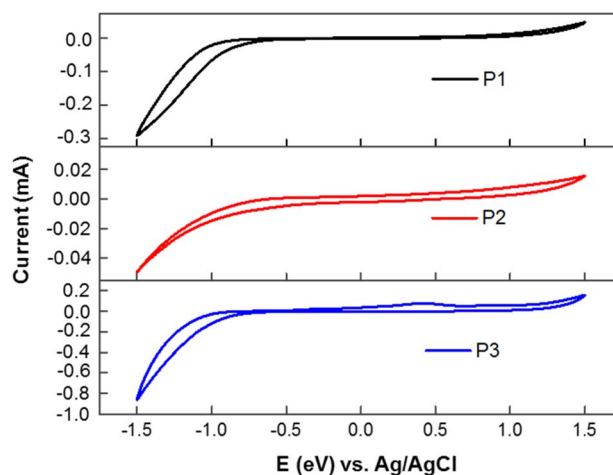


Fig. 2 Cyclic voltammograms of homopolymers P1, P2, and P3 measured in a 0.1 M solution of TBAPF₆ in acetonitrile at a scan rate of 50 mV s⁻¹.



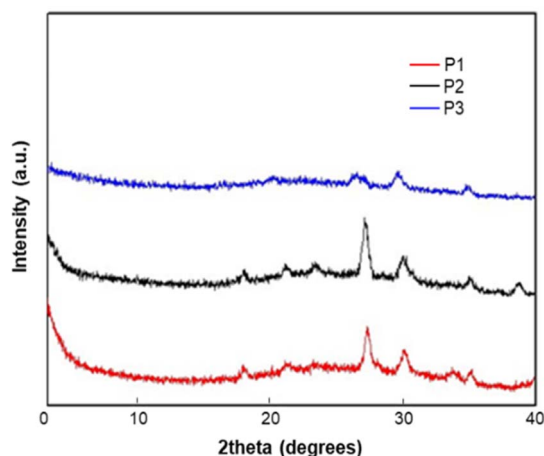


Fig. 3 X-ray diffraction (XRD) patterns of P1, P2 and P3. Films for XRD measurement were prepared by drop casting in CHCl_3 (10 mg ml^{-1} of solvent) on the silicon substrate.

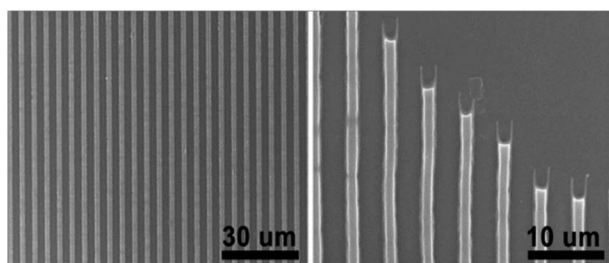


Fig. 4 SEM image of the wire patterns of P1 created by EMAN.

($\sim 580 \text{ nm}$). In comparison to the optical properties of the synthesized polymers and PCBM, we find that they are similar to PCBM optical properties which were published earlier.⁵⁵ All the absorption spectra of P1, P2 and P3 show bandgaps in the range 2.13–2.08 eV similar to PCBM too.

Cyclic voltammetry (CV) measurement was performed on potentiostat/galvanostat (SP-150 OMA Company). The

supporting electrolyte was tetrabutylammonium hexafluorophosphate (TBAPF6) in acetonitrile (0.1 M) at a scan rate 50 mV s^{-1} . A three-electrode cell was used and Pt wire and Ag/AgCl [Ag in 0.1 M KCl] were used as the counter and reference electrodes, respectively. The (E_{HOMO} and E_{LUMO}) of the homopolymers were determined from the following relationships: $E_{\text{HOMO}} = -(E_{\text{oxd}} + 4.72) \text{ eV}$ and $E_{\text{LUMO}} = -(E_{\text{red}} + 4.72) \text{ eV}$. Where E_{oxd} and E_{red} are the onset oxidation and reduction potentials of the polymers vs. the Ag/AgCl reference electrode, respectively. The polymer films were drop-casted from polymer–chloroform solution on ITO glass slides, *ca.* 10 mg ml^{-1} . The voltammograms of polymers P1, P2, and P3 versus SCE are shown in Fig. 2. Energy levels were estimated using the onset of the reduction peak (LUMO level) and the onset of the oxidation peak (HOMO level), assuming that the SCE is -4.72 eV from the vacuum. The results obtained are summarized in Table S2.[†] Energy levels of polymers P1, P2 and P3 are relatively low with LUMO energy levels in the range of -3.72 to -3.89 eV , a value that is close to that of PC₆₁BM. The LUMO energy level of polymer P1 was found to be at -3.74 eV . HOMO energy levels are also low with a value of -5.64 and -5.61 eV for both P1 and P2 and -5.64 eV for P3. However, these three polymers show no electrochemical reversibility in the oxidation and reduction processes.

XRD study of homopolymers P1, P2 and P3

The X-ray diffraction (XRD) of the homopolymers P1–P3 was measured from their thin-film casting on the silicon substrate (Fig. 3). All polymers did not show any peaks in the narrow-angle region, which indicates there is no arrangement of the alkyl chain in the solid state. The diffraction peaks at $2\theta = 17.99^\circ$ (4.98 \AA), and 28.01° (3.28 \AA) for P1; 18.00° (4.98 \AA), and 28.01° (3.28 \AA) for P2; and 27.31° (3.39 \AA) for P3 are attributed to π – π stacking between polymer chains. The XRD results implied that all the polymers possess a good arrangement in the solid state because of the π – π stacking between the polymer units. The differences in the peak intensities between these polymers indicate that the crystallinity in the solid-state is related to the

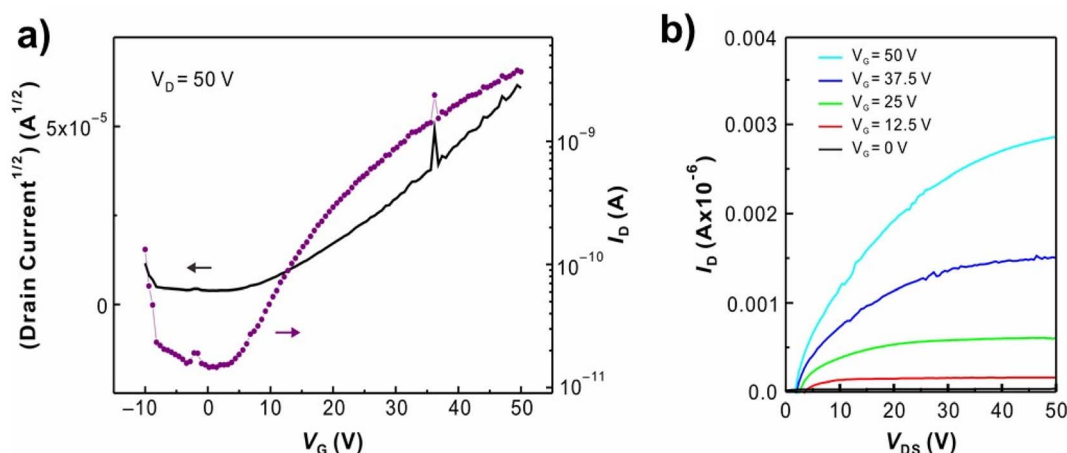


Fig. 5 Representative (a) transfer and (b) output curves of FET device using P1 show electron mobility of $2.11 \times 10^{-3} \text{ cm}^2 \text{ s}^{-1} \text{ V}^{-1}$.



backbone and alkyl substitutions of the backbone, which will affect the uniformity of film and the device performance.

Field-effect mobility study of homopolymer P1, P2, and P3

The field-effect mobility of P1 was investigated. Due to the rigid planarity, P1 has low solubility in most common organic solvents which hamper the fabrication of FET devices by using conventional processes. As addressing this issue, the eutectic-melt-assisted nanoimprinting (EMAN)^{49–54} method was applied to create FET devices using polymer P1. Briefly, wire patterns of P1 with 1.5 $\mu\text{m}/3.0 \mu\text{m}$ line and space were first created by EMAN (Fig. 4), and then they were transferred on a highly doped silicon wafer with a thermally grown 200 nm thick oxide layer. Subsequently, 200 nm thick gold electrodes separated by 100 μm were deposited through a showdown mask on the wire patterns. Current–voltage (I – V) characteristics of the fabricated FET devices were measured using bottom-gate geometry, and the saturation regime mobility was calculated. As shown in Fig. 5, the transfer and output curves of polymer P1 show n-type characteristics. Similar to other n-type semiconductors, a large hysteresis was observed.^{56–58} The calculated saturation electron mobility is $2.11 \times 10^{-3} \text{ cm}^2 \text{ s}^{-1} \text{ V}^{-1}$, which is comparable to the electron mobility of PC₆₁BM.^{59,60} FET devices based on polymer P2 and P3 were also prepared by EMAN. Because of poor film morphology or poor adhesion problem (ESI Fig. S10 and S11†), both P2 and P3-based FET devices didn't successfully work.

Conclusions

We have successfully synthesized homopolymers P1, P2 and P3 presenting n-type properties for potential applications as acceptor polymers. The homopolymers were synthesized using the CH–CH arylation polymerization in an eco-friendly one-step coupling reaction which reduces the number of steps necessary to obtain these polymers, respectively. These polymers possess low lying HOMO and LUMO levels. Also, their electron mobilities were tested and the resulting electron mobility was as high as $2.11 \times 10^{-3} \text{ cm}^2 \text{ s}^{-1} \text{ V}^{-1}$ which is comparable to that of PCBM. These polymers are promising features for applications as acceptors in all-polymer solar cells and transistors and will be further investigated in the future.

Author contributions

G. M. Nassar: conceptualization, methodology, formal analysis, investigation, visualization, writing – original draft, review & editing. J. Chung: methodology, formal analysis, investigation, writing – review & editing. C. K. Trinh: formal analysis, investigation, writing – review & editing. A. A. El-Shehawey: writing – review & editing. A. A. El-Barbary: writing – review & editing. Y. Kang: writing – review & editing. Supervisor J.-S. Lee: writing – review & editing, resources, supervision.

Conflicts of interest

There are no conflicts to declare.

Acknowledgements

This research was supported by the Samsung Research Funding Center of Samsung Electronics under Project Number SRFC-MA1502-11. We would like to thank Van Lang University, Vietnam for the support for this research.

Notes and references

- 1 Y. Li, C.-Y. Gao, X.-H. Fan and L.-M. Yang, *J. Chem. Eng.*, 2022, **443**, 136536.
- 2 S. Yin, W. Lu, R. Wu, W. Fan, C.-Y. Guo and G. Chen, *ACS Appl. Mater. Interfaces*, 2020, **12**, 3547–3553.
- 3 C. Fradin, F. Guittard, I. F. Perepichka and T. Darmanin, *Electrochim. Acta*, 2022, **425**, 140684.
- 4 O. A. Kraevaya, A. F. Latypova, A. A. Sokolova, A. A. Seleznyova, N. A. Emelianov, N. A. Slesarenko, V. Y. Markov, L. A. Frolova and P. A. Troshin, *Sustainable Energy Fuels*, 2022, **6**, 3485–3489.
- 5 L. Papammagri, S. R. Agnihotra, N. Maohar, R. M. Bouldin and S. K. Manohar, *Macromolecules*, 2021, **54**, 1507–1516.
- 6 M. Seike, M. Uda, T. Suzuki, H. Minami, S. Higashimoto, T. Hirai, Y. Nakamura and S. Fujii, *ACS Omega*, 2022, **15**, 13010–13021.
- 7 Y.-Z. Chen, J.-G. Fu, X.-M. Ji, S.-S. Zhang and C.-G. Feng, *Chem. Commun.*, 2022, **58**, 6661–6664.
- 8 C. K. Trinh, G. M. Nassar, N. I. Abdo, S. Jung, W. Kim, K. Lee and J.-S. Lee, *RSC Adv.*, 2022, **12**, 17682–17688.
- 9 S. Xu, E. H. Kim, A. Wei and E.-I. Negishi, *Sci. Technol. Adv. Mater.*, 2014, **15**, 044201–044223.
- 10 F. Babudri, G. M. Farinola and F. Naso, *J. Mater. Chem.*, 2004, **14**, 11–34.
- 11 T. J. Aldrich, A. S. Dudnik, N. D. Eastham, E. F. Manley, L. X. Chen, R. P. H. Chang, F. S. Melkonyan, A. Facchetti and T. J. Marks, *Macromolecules*, 2018, **51**, 9140–9155.
- 12 Y. Sui, Y. Shi, Y. Deng, R. Li, J. Bai, Z. Wang, Y. Dang, Y. Han, N. Kirby, L. Ye and Y. Geng, *Macromolecules*, 2020, **53**, 10147–10154.
- 13 V. Dichiarante, M. Fagnoni and A. Albin, *Angew. Chem., Int. Ed.*, 2007, **46**, 6495–6498.
- 14 T. Jia, A. Bellomo, S. Montel, M. Zhang, K. EL Baina, B. Zheng and P. J. Walsh, *Angew. Chem., Int. Ed.*, 2014, **53**, 260–264.
- 15 N. I. Abdo, J. Ku, A. A. El-Shehawey, H.-S. Shim, J.-K. Min, A. A. El-Barbary, Y. H. Jang and J.-S. Lee, *J. Mater. Chem. A*, 2013, **35**, 10306–10317.
- 16 W. Elsayy, H. Kang, K. Yu, A. El-Barbary, K. Lee and J.-S. Lee, *J. Polym. Sci., Part A: Polym. Chem.*, 2014, **52**, 2926–2933.
- 17 M. Shaker, J.-H. Lee, C. K. Trinh, W. Kim, K. Lee and J.-S. Lee, *RSC Adv.*, 2015, **5**, 66005–66012.
- 18 M. Shaker, C. K. Trinh, W. Kim, K. Lee and J.-S. Lee, *New J. Chem.*, 2015, **39**, 4957–4964.
- 19 C. K. Trinh, J.-H. Lee, J. Choi, M. Shaker, W. Kim and J.-S. Lee, *New J. Chem.*, 2018, **42**, 2557–2563.
- 20 Y.-S. Yang, S. Lee, S. H. Son, H.-S. Yoo, Y. H. Jang, J.-W. Shin, H.-J. Won, J. Sim and N.-J. Kim, *Org. Chem. Front.*, 2022, **9**, 5906–5911.



- 21 F. D'Amico, C. Papucci, D. Franchi, G. Reginato, M. Calamante, L. Zani, A. Dessi and A. Mordini, *ACS Sustainable Chem. Eng.*, 2022, **10**(9), 3037–3047.
- 22 A. Ichige, H. Saito, J. Kuwabara, T. Yasuda, J.-C. Choi and T. Kanbara, *Macromolecules*, 2018, **51**, 6782–6788.
- 23 C. Y. K. Chan, N.-W. Tseng, J. W. Y. Lam, J. Liu, R. T. K. Kwok and B. Z. Tang, *Macromolecules*, 2013, **46**, 3246–3256.
- 24 Y. Yue, J. Peng, D. Wang, Y. Bian, P. Sun and C. Chen, *J. Org. Chem.*, 2017, **82**, 5481–5486.
- 25 P.-Y. Lee, P. Liang and W.-Y. Yu, *Org. Lett.*, 2017, **19**, 2082–2085.
- 26 S. Rej and N. Chatani, *Angew. Chem., Int. Ed.*, 2022, **61**, e202209539–e202209556.
- 27 S. Rej, A. Dasa and N. Chatani, *Chem. Sci.*, 2021, **12**, 11447–11454.
- 28 C. S. Yeung and V. M. Dong, *Chem. Rev.*, 2011, **111**, 1215–1292.
- 29 S. A. Girard, T. Knauber and C.-J. Li, *Angew. Chem., Int. Ed.*, 2014, **53**, 74–100.
- 30 Y. Wu, J. Wang, F. Mao and F. Y. Kwong, *Chem.–Asian J.*, 2014, **9**, 26–47.
- 31 I. Osaka, T. Abe, S. Shinamura, E. Miyazaki and K. Takimiya, *J. Am. Chem. Soc.*, 2010, **132**, 5000–5001.
- 32 S. Fratini, M. Nikolka, A. Salleo, G. Schweicher and H. Sirringhaus, *Nat. Mater.*, 2020, **19**, 491–502.
- 33 G. Yu, J. Gao, J. C. Hummelen, F. Wudl and A. J. Heeger, *Science*, 1995, **270**, 1789–1791.
- 34 A. Chaudhary, D. K. Pathak, M. Tanwar, P. Yogi, P. R. Sagdeo and R. Kumar, *ACS Appl. Electron. Mater.*, 2019, **1**, 58–63.
- 35 J. J. M. Halls, C. A. Walsh, N. C. Greenham, E. A. Marseglia, R. H. Friend, S. C. Moratti and A. B. Holmes, *Nature*, 1995, **376**, 498–500.
- 36 Y. Kim, S. Cook, S. A. Choulis, J. Nelson, J. R. Durrant and D. D. C. Bradley, *Chem. Mater.*, 2004, **16**, 4812–4818.
- 37 M. Liao, J. Duan, P. Peng, J. Zhang and M. Zhou, *RSC Adv.*, 2020, **10**, 41764–41779.
- 38 Y. Jiang, J. Chen, Y. Sun, Q. Li, Z. Cai, J. Li, Y. Guo, W. Hu and Y. Liu, *Adv. Mater.*, 2019, **31**, 1805761.
- 39 J. Ge, B. Ding, S. Hou, M. Luo, D. Nam, H. Duan, H. Gao, Y. C. Lam and H. Li, *Nat. Commun.*, 2021, **12**, 3146.
- 40 L. Ackermann, *Chem. Rev.*, 2011, **111**, 1315–1345.
- 41 T. Satoh and M. Miura, *Chem. Lett.*, 2007, **36**, 200–205.
- 42 M. Lafrance and K. Fagnou, *J. Am. Chem. Soc.*, 2006, **128**, 16496–16497.
- 43 N. I. Abdo, A. A. El-Shehawy, A. El-Barbary and J.-S. Lee, *Eur. J. Org. Chem.*, 2012, **28**, 5540–5551.
- 44 M. Wakioka, N. Ichihara, Y. Kitano and F. Ozawa, *Macromolecules*, 2014, **47**, 626–631.
- 45 X. Jie, Y. Shang, P. Hu and W. Su, *Angew. Chem., Int. Ed.*, 2013, **52**, 3630–3633.
- 46 Y. Yang, J. Lan and J. You, *Chem. Rev.*, 2017, **117**, 8787–8863.
- 47 D. Alberico, M. E. Scott and M. Lautens, *Chem. Rev.*, 2007, **107**, 174–238.
- 48 I. V. Seregin and V. Gevorgyan, *Chem. Soc. Rev.*, 2007, **36**, 1173–1193.
- 49 J. K. Hwang, *Nat. Nanotechnol.*, 2010, **5**, 742–748.
- 50 J. Chung, J. Hyon, K.-S. Park, B. Cho, J. Baek, J. Kim, S. U. Lee, M. M. Sung and Y. Kang, *Sci. Rep.*, 2016, **6**, 1–11.
- 51 Q. Zhang, K. D. O. Vigier, S. Royer and F. Jérôme, *Chem. Soc. Rev.*, 2012, **41**, 7108–7146.
- 52 D. Carriazo, M. C. Serrano, M. C. Gutiérrez, M. L. Ferrera and F. d. Monte, *Chem. Soc. Rev.*, 2012, **41**, 4996–5014.
- 53 C. Bathula, S. Jeong, J. Chung and Y. Kang, *J. Nanosci. Nanotechnol.*, 2016, **16**, 2796–2799.
- 54 J. Kim, J. Chung, J. Hyon, T. Kwon, C. Seo, J. Nam and Y. Kang, *Chem. Commun.*, 2014, **50**, 10258–10261.
- 55 S. Cook, H. Ohkita, Y. Kim, J. J. Benson-Smith, D. D. C. Bradley and J. R. Durrant, *Chem. Phys. Lett.*, 2007, **445**, 276–280.
- 56 W. Xu and S.-W. Rhee, *Org. Electron.*, 2011, **12**, 2040–2046.
- 57 W. Xu and S.-W. Rhee, *Org. Electron.*, 2010, **11**, 836–845.
- 58 Y. Ni, Y. Wang and W. Xu, *Small*, 2021, **17**, 1905332.
- 59 E. V. Hauff, V. Dyakonov and R. Parisi, *Sol. Energy Mater. Sol. Cells*, 2005, **87**, 149–152.
- 60 C. Waldauf, P. Schilinsky, M. Perisutti, J. Hauch and C. J. Brabec, *Adv. Mater.*, 2003, **15**, 2084–2088.

